

1 Outer organic layer and internal repair mechanism protects 2 pteropod *Limacina helicina* from ocean acidification

3

4 **Victoria L Peck¹, Geraint A Tarling¹, Clara Manno¹, Elizabeth M Harper², Eithne**
5 **Tynan³.**

6 1. British Antarctic Survey, High Cross, Madingley Rd, Cambridge, CB5 8NP, UK

7 2. Department of Earth Sciences, University of Cambridge, Downing Street, Cambridge,
8 CB2 3EQ, UK

9 3. Ocean and Earth Science, National Oceanography Centre Southampton, University of
10 Southampton Waterfront Campus, European Way, Southampton SO14 3ZH, UK

11

12 **Scarred shells of polar pteropod *Limacina helicina* collected from the Greenland Sea in**
13 **June 2012 reveal a history of damage, most likely failed predation, in earlier life stages.**
14 **Evidence of shell fracture and subsequent re-growth is commonly observed in**
15 **specimens recovered from the sub-Arctic and further afield. However, at one site within**
16 **sea-ice on the Greenland shelf, shells that had been subject to mechanical damage were**
17 **also found to exhibit considerable dissolution. It was evident that shell dissolution was**
18 **localised to areas where the organic, periostracal sheet that covers the outer shell had**
19 **been damaged at some earlier stage during the animal's life. Where the periostracum**
20 **remained intact, the shell appeared pristine with no sign of dissolution. Specimens**
21 **which appeared to be pristine following collection were incubated for four days.**
22 **Scarring of shells that received periostracal damage during collection only became**
23 **evident in specimens that were incubated in waters undersaturated with respect to**
24 **aragonite, $\Omega_{Ar} \leq 1$. While the waters from which the damaged specimens were collected**
25 **at the Greenland Sea sea-ice margin were not $\Omega_{Ar} \leq 1$, the water column did exhibit the**
26 **lowest Ω_{Ar} values observed in the Greenland and Barents Seas, and was likely to have**
27 **approached $\Omega_{Ar} \leq 1$ during the winter months. We demonstrate that *L. helicina* shells are**
28 **only susceptible to dissolution where both the periostracum has been breached and the**
29 **aragonite beneath the breach is exposed to waters of $\Omega_{Ar} \leq 1$. Exposure of multiple layers**
30 **of aragonite in areas of deep dissolution indicate that, as with many molluscs, *L. helicina***
31 **is able to patch up dissolution damage to the shell by secreting additional aragonite**

32 **internally and maintain their shell. We conclude that, unless breached, the**
33 **periostracum provides an effective shield for pteropod shells against dissolution in**
34 **waters $\Omega_{Ar} \leq 1$, and when dissolution does occur the animal has an effective means of**
35 **self-repair. We suggest that future studies of pteropod shell condition are undertaken**
36 **on specimens from which the periostracum has not been removed in preparation.**

37

38 **Key words**

39 Limacina helicina

40 Ocean acidification

41 Periostracum

42 Greenland

43 Sea ice

44 Pteropod

45

46

47

48

49

50

51

52

53

54

55

56

57

58

59

60 INTRODUCTION

61 Since the start of the Industrial Revolution, about 48% of the anthropogenic CO₂ emitted to
62 the atmosphere has been sequestered into the world's oceans (Sabine et al., 2004). This
63 excess CO₂ is dissolved into the surface ocean and reacts with seawater, causing pH and
64 dissolved carbonate ion concentrations, [CO₃²⁻], to fall, a phenomenon commonly referred to
65 as ocean acidification (Caldeira & Wickett, 2003; Orr et al., 2005). In the polar-regions,
66 ocean acidification is further exacerbated by increased solubility of gases within colder
67 waters (Fabry et al., 2009) and also by sea ice processes, which can amplify seasonal
68 variability in saturation state of mixed layer waters (Fransson et al., 2013). Furthermore,
69 increased ice melt is freshening the mixed layer, lowering Total Alkalinity (TA) and
70 Dissolved Inorganic Carbon (DIC) concentration. Carbonate saturation of polar waters is
71 rapidly falling to values where aragonite, the less stable form of calcium carbonate (Mucci,
72 1983), becomes susceptible to dissolution ($\Omega_{Ar} \leq 1$; Orr et al., 2005). Pteropods, or 'sea
73 butterflies', are pelagic gastropods which have evolved 'wings' derived from the foot
74 enabling them to swim. The delicate shells of pteropods are made of the metastable aragonite
75 and thus may be particularly prone to dissolution.

76 The true polar pteropod, *Limacina helicina*, is a keystone species within polar ecosystems
77 (Lalli & Gilmar 1989; Comeau et al., 2009; Hunt et al., 2008; Hunt et al., 2010). Living in the
78 upper few hundred meters of the water column, in waters which are becoming increasingly
79 undersaturated with respect to aragonite, *L. helicina* is frequently presented as being the
80 "canary in the coal mine" for ocean acidification (e.g. Orr et al., 2005). Incubation
81 experiments, investigating the response of the Arctic sub-species *L. helicina helicina* (Hunt et
82 al., 2010) to elevated pCO₂ scenarios indicate reduced net calcification (Comeau et al., 2010)
83 and degradation in shell condition in undersaturated waters (Lischka et al., 2011).
84 Observations of living specimens collected from a region of upwelling in the Southern
85 Ocean, suggest that Antarctic sub-species *L. helicina antarctica* (Hunt et al., 2010) is subject
86 to extensive dissolution where $\Omega_{Ar} = 1$ (Bednarsek et al., 2012a). However, many species of
87 mollusc thrive with undersaturated waters, for example within freshwater or deep-sea
88 hydrothermal vent communities, on account of their calcareous shells being protected from
89 dissolution by the presence of a protective organic coating, a periostracum, covering their
90 shells (Taylor & Kennedy, 1969; Harper, 1997). Possession of a periostracum is a shared

91 character for all shelled molluscs (Harper, 1997). This thin organic sheet of the periostracum
92 is secreted at the edge of the mantle and is the first formed layer of the shell. The primary
93 function of the periostracum is to separate the site of calcification from the ambient water and
94 to provide the initial template onto which the shell is crystallised. It is this isolation of the
95 extrapallial space by the periostracum that allows calcification to occur within waters which
96 are undersaturated with respect to carbonate, with extreme examples being the occurrence of
97 molluscs within hydrothermal vent (e.g. Tunnicliffe et al., 2009) and freshwater
98 environments (e.g. Harper, 1997). A secondary function of the periostracum is to provide a
99 protective veneer shielding the shell from the corrosive effects of undersaturated waters or
100 chemical attack from predators (Harper, 1997). Of critical note, since the periostracum is only
101 formed at the actively growing shell margin (Saleuddin & Petit 1983), thinning or loss of the
102 periostracum via physical and biotic abrasion, epibiont erosion and bacterial decay will limit
103 its effectiveness as protection as there is no possibility of repairing it once it is damaged.

104 Although there has been very little published on biomineralization in pteropods, it is clear
105 from the shell microstructure (Bandel, 1990) that they follow the typical molluscan pattern.
106 In the case of *Limacina* the shell is composed of well ordered crossed-lamellar and prismatic
107 aragonite layers, internal to an ultra-thin ($<1 \mu\text{m}$) periostracum (Sato-Okoshi et al., 2010).
108 The findings of Bednarsek et al. (2012a, 2012b) seem to suggest that pteropods receive little
109 benefit from their periostracum when exposed to undersaturated waters. Quantification of
110 pteropod shell loss by Bednarsek et al (2014a), found that 14 day exposure to undersaturated
111 waters ($\Omega_{\text{Ar}} = 0.8$) resulted in a shell loss of $17.1\% \pm 3.0\%$. While the rate of dissolution
112 reported by Bednarsek et al (2014a) is less than that predicted for the dissolution rate of pure
113 aragonite, the fact that dissolution was reported over the entirety of the shells, questions the
114 effectiveness of the periostracum for *L. helicina antarctica*. However, we note that Bednarsek
115 et al. (Bednarsek et al., 2012a; Bednarsek et al., 2012c; Bednarsek et al., 2014b; Bednarsek et
116 al., 2015) used chemical and plasma etching methods on shells prior to imaging, with the
117 intention of removing the periostracum. Given the protective role of the periostracum in other
118 shelled molluscs living in undersaturated waters, we opt to examine the relationship between
119 dissolution and periostracal cover on specimens that are not subject to any preparation steps
120 that would compromise the condition of the periostracum or the shell beneath. Our minimal
121 preparation approach intends to establish how effective the periostracum is in protecting the
122 shells of pteropods.

123 Here we present our observations of *L. helicina helicina* shells collected from the Greenland
124 and Barents Seas in June 2012 and the result of a small scale incubation experiment to assess
125 the effectiveness of the periostracum, and therefore vulnerability, of this species to ocean
126 acidification in the Arctic.

127

128 **METHODS**

129 This study carried out observations and incubations on *L. helicina helicina* specimens
130 recovered during routine motion-compensated plankton net deployments during research
131 cruise JR271 on board RRS *James Clark Ross* in June-July 2012. *L. helicina helicina*
132 specimens were recovered at three sites within the Greenland and Barents Seas as detailed in
133 Table 1 and Figure 1.

134 **Water column structure and chemistry and manipulation of seawater for incubation**

135 Vertical CTD profiles were performed to characterise important water column structure
136 (temperature, salinity, Chl-a) and carbonate chemistry. The depth of water collection for the
137 experimental setup was then determined based on these initial profiles. The unfiltered water
138 was collected from dedicated CTD casts and transferred to acid-cleaned clear 1 L Duran
139 bottles and then sealed pending carbonate chemistry manipulation and the addition of
140 pteropods. Subsamples at time zero were taken directly from the CTD and immediately
141 measured for Total Alkalinity (TA) and Dissolved Inorganic Carbon (DIC) to characterise the
142 water column structure. DIC was analysed with an Apollo SciTech CT analyser (AS-C3),
143 which uses a CO₂ infrared detector (LICOR 7000). TA was determined using a semiclosed-
144 cell titration (Dickson et al., 2007) within the Apollo SciTech's AS-ALK2 Alkalinity
145 Titrator. For both TA and DIC, the precision was 0.1% or better, with accuracy verified using
146 certified reference materials (A.G. Dickson, Scripps). The remaining variables of the
147 carbonate system were calculated with the CO2SYS programme (version 1.05, Lewis &
148 Wallace, 1998; Pierrot et al., 2006), using the constants of Mehrbach et al. (1973) refitted by
149 Dickson & Millero (1987). Carbonate chemistry in the experimental bottles was subsequently
150 manipulated using equimolar additions of acid (HCl, 1 mol L⁻¹) and HCO₃⁻ (1 mol L⁻¹), as
151 recommended by Gattuso et al. (2010) for increasing DIC at constant TA. The volumes of
152 HCl and HCO₃⁻ required to adjust *p*CO₂ to the chosen target values (650 µatm, 800 µatm)

153 were calculated from the measured ambient state of the carbonate system in seawater using
154 CO2SYS. A further set of bottles remained unmanipulated (ambient). The bottles were sealed
155 until the pteropods were added.

156 **Pteropod collection.**

157 A motion compensated Bongo net, with mesh sizes of 100 μm and 200 μm was deployed at
158 dawn to 200 m below the sea surface and hauled vertically. Samples were gently transferred
159 into a bucket of ambient seawater within which pteropods were found to settle to the bottom
160 and could then be easily collected with a wide-mouthed plastic pipette. Visual examination of
161 specimens under an Olympus SZX16 identified those that were actively swimming and had
162 intact, fully translucent shells. Specimens that (i) had not yet developed wings (and moved
163 via cilia), (ii) were winged but not actively swimming within one hour of collection or (iii)
164 did not have fully translucent shells, were rinsed with pH-buffed de-ionised water to induce
165 mortality. Of these non-living specimens, all specimens within categories (i) and (ii) as well
166 as a representative selection of category (iii) were preserved by air drying and stored in
167 individual wells within specimen slides.

168 **Pteropod incubation**

169 Actively swimming juvenile specimens which appeared to have fully-translucent and intact
170 shells were acclimatised to laboratory conditions in ambient seawater for about 4 hours as the
171 incubation bottles were prepared. Five specimens were then randomly distributed into each of
172 the three pre-prepared Duran bottles (see above). Six of the winged-specimens with fully
173 translucent shells in which mortality was induced within one hour of collection were also
174 incubated in ambient conditions and under elevated levels of $p\text{CO}_2$ and were treated in an
175 identical way to the actively swimming specimens to provide a control. These non-living
176 specimens were divided between an additional three incubation bottles, two specimens per
177 bottle.

178 Incubation bottles were stored in the dark within a cold room set to $\sim -1.5^\circ\text{C}$, the same
179 temperature as the ambient sea water within the mixed layer below the sea ice. During the
180 incubation, bottles were inspected daily to ensure the living specimens were actively
181 swimming. Each bottle was gently inverted, observed for several minutes and replaced.

182 At the end of the 4 day incubation, a subsample of water was collected from each
183 manipulated bottle for TA and DIC to determine the true $p\text{CO}_2$ values achieved by the
184 manipulation and also to determine the saturation state with respect to aragonite, Ω_{Ar} . Care
185 was taken not to collect any pteropods in this water sample and not to generate any bubbles
186 during the transfer. 5 ml of this water was then removed from the sample, 250 μl of mercuric
187 chloride was added and the bottle was sealed prior to analysis. Following collection of the
188 DIC and TA sample, water was gently decanted out of the Duran bottles into deep walled
189 glass Petri dishes. Each full dish was inspected under the light microscope and pteropods
190 were removed by gentle pipetting.

191 **Pteropod shell analysis**

192 Once all specimens were recovered from each treatment bottle, they were observed using an
193 Olympus SZX16 with a mounted Canon D5 camera to document their vitality/mobility. All
194 specimens were then individually rinsed in pH-buffered ultra-pure water three times before
195 being placed in a specimen slide and air-dried. Once dried, specimens were photographed
196 again under the light microscope onboard, prior to storage for transport within air-tight
197 containers containing silica-gel sachets.

198 Specimens were imaged under scanning electron microscope at the Natural History Museum,
199 London. As the specimens were free of sea salts and dry, no preparation was required prior to
200 imaging with a LEO 1455 variable pressure SEM. Higher magnification and resolution
201 images were generated by use of the Ultra Plus SEM. Specimens were imaged without a
202 coating using the Ultra Plus SEM, but the best images were generated by specimens coated in
203 ~ 10 nm of gold-palladium in a sputter-coater.

204

205 **RESULTS**

206 **Water column chemistry**

207 Temperature, salinity and Ω_{Ar} as measured from CTD casts at each site (Table 1) are shown
208 in Fig. 2. While the upper 200 m of the two open water sites in the Greenland Sea and the
209 Barents Sea exhibit similar temperature and salinity profiles, typical of a well mixed upper
210 water column, the Greenland Sea ice margin site exhibited strong thermo-halocline

211 stratification above 200 m. At the Greenland ice margin site, temperature decreased from
212 $\sim 3^{\circ}\text{C}$, similar to the open ocean water sites to $\sim -1.6^{\circ}\text{C}$ beneath the sea ice within the upper
213 200 m. Freshening of the surface water column due to sea ice melt was also evident, with
214 salinity falling below 33 within the upper 20 m. While Ω_{Ar} values at the Greenland Sea ice
215 margin were the lowest measured within the scientific cruise (Tyrrell et al., this issue), Ω_{Ar}
216 exceeded 1 at all three sites, meaning that the water column at each site was oversaturated
217 with respect to aragonite at the time of measurement.

218 **Specimens recovered**

219 At the Greenland Sea ice margin, 56 specimens of *L. helicina helicina* were recovered in the
220 two deployments of the Bongo net. Analysis of their maximum shell diameter identified two
221 distinct cohorts of *L. helicina helicina* at the Greenland Sea ice margin (Fig 3). The smaller
222 cohort had an average maximum shell diameter of $202 \pm 35 \mu\text{m}$ (n=20). These specimens
223 were veligers that had developed one whorl (Fig. 4 V1 and V2) and were ciliated, having not
224 yet developed wings. The larger cohort, consisting of juveniles, had an average maximum
225 shell diameter of $1255 \pm 146 \mu\text{m}$ (n=36), and had typically developed 3-4 whorls (Fig. 4 J1-
226 J6). The juvenile specimens had also developed wings, were active swimmers, and were far
227 more agile than the veligers.

228 Further specimens of *L. helicina helicina*, including 20 adults with maximum shell
229 diameters ranging in size from 4.8 to 8.2 mm, were recovered from the Greenland Sea and
230 Barents Sea open water sites to the east on the 21st and 23rd of June 2015 (Fig. 1).

231 **Shell analysis**

232 On board, light microscope examination of specimens collected at the open water sites
233 (Greenland Sea and Barents Sea) found all shells were fully translucent. Although evidence
234 of fracture and regrowth was apparent in several shells recovered from both of these sites
235 (Fig. 5), the shell on both sides of the fracture remained fully translucent. At the Greenland
236 Sea ice margin, all veligers also exhibited fully-translucent shells (Fig. 4, V1-2), but juvenile
237 specimens did not all present fully translucent shells (Fig. 4, J1-2) with 13 out of 36 juveniles
238 exhibiting areas of shell that appeared opaque under light microscope (Fig. 4, J3-6). Three of
239 these specimens presented deep damage to the shell surface (Fig. 4, J5- 6). Investigation of

240 areas which appeared to be opaque under light microscope with SEM revealed three types of
241 shell damage.

242 **(i) Central whorls**

243 85% of the damaged juveniles recovered from the Greenland Sea ice margin exhibited
244 damage to the central whorl. SEM analysis showed that the areas of opaque shell within the
245 central whorl of J3 and J4 corresponded to regions of finely pitted surface texture through to
246 fully exposed aragonite crystals (Fig. 6).

247 **(ii) Deep damage**

248 23% of the damaged juveniles recovered from the Greenland Sea ice margin exhibited deep
249 damage to their shell, meaning that although the shell was not observed to be perforated,
250 dissolution appeared to have removed at least one layer of aragonite. In the case of J5 (Fig. 7
251 b-e) and J6 (Fig. 8 b-e), deeper damage to the shell was clearly identifiable under SEM with
252 extensive exposure of multiple aragonite layers visible. The progressive exposure of
253 numerous layers of aragonite was evident in both specimens to a depth that exceeded the
254 thickness of the original shell (Fig. 7a). In each case the margin between the area of exposed
255 aragonite and translucent, smooth shell was abrupt. The growth of the subsequent whorls can
256 be seen to mould around the deep damage of inner whorls (Fig. 7e, Fig. 8c).

257 **(iii) Fracture zones**

258 62% of the damaged specimens removed from the Greenland Sea ice margin exhibited
259 fracture zone damage. SEM analysis of opaque linear features extending across the whorls of
260 J5 and J6 revealed dissolution of aragonite along a fracture of the original shell and
261 subsequent growth of new shell (Fig. 7a, b, f, g, and Fig, 8a, b, e and f). With J5 it appears
262 that dissolution at the fracture zone is restricted to the new shell (Fig. 7 f,g). Under high
263 magnification using the Ultra Plus SEM, the area of exposed aragonite crystals on the new
264 section of shell (closest to the fracture) clearly revealed a loose section of a filmy layer that
265 appeared to extend across the new, fully opaque section of shell, but was not present over the
266 area of exposed aragonite (Fig. 7g, h). On J6, the dissolution appeared to be concentrated on
267 the old shell side of the fracture (Fig. 8 e, f). The uncoated specimens within the Ultra Plus
268 SEM did not generate such crisp images as the coated specimens, but nonetheless a filmy

269 layer with perforations overlaying what appear to be vertically stacked, partially eroded
270 aragonite crystals can be seen (Fig. 8f).

271 **Incubations**

272 Actively swimming specimens of *L. helicina* with fully translucent shells collected from the
273 Greenland Sea ice margin on June 18th 2012 were incubated for 4 days under the treatments
274 shown in Table 2.

275 Although the simulated $p\text{CO}_2$ manipulations did not achieve their target values, both sets of
276 treatments (650 μatm and 800 μatm) resulted in conditions undersaturated with respect to
277 aragonite, with Ω_{Ar} values of 0.76 and 0.63 respectively. After four days of incubation, there
278 were no fatalities in any of the treatments.

279 Inspection of the shells at the end of the incubation revealed that all shells within the ambient
280 treatment (n=5) remained fully translucent (Fig 9a). At the end of the incubations in which
281 $p\text{CO}_2$ was elevated, opaque regions to the shell had developed in 2 of the 5 specimens at a
282 target $p\text{CO}_2$ of 650 μatm (Fig. 9b), and 3 of the 5 specimens at a target $p\text{CO}_2$ of 800 μatm
283 (Fig. 9c). These opaque areas were superficial, compared to the damage observed in the 13
284 non-pristine specimens recovered from the Greenland Sea ice margin.

285 The shells of non-living specimens that were incubated with ambient water and at a target
286 $p\text{CO}_2$ of 650 μatm (Fig. 9d and e respectively) for 4 days became uniformly opaque.

287

288 **DISCUSSION**

289 We observed naturally occurring dissolution to the juvenile shells of *L. helicina helicina*
290 recovered at the Greenland Sea ice margin. It is evident that shell dissolution is exclusively
291 associated with areas where damage to the protective periostracal sheet has been sustaining
292 during the animal's life. Some areas of damage extend deeper than the original thickness of
293 the shell, indicating that the animals respond to shell damage by secreting aragonite internally
294 to maintain their shells. Where the periostracum remained fully intact, the shell appears
295 pristine (fully translucent) with no sign of dissolution. Recently acquired periostracal damage
296 associated with collection, becomes evident by the early stages of shell dissolution after four
297 days of incubation, but only in waters $\Omega_{\text{Ar}} < 1$.

298 As is typical of the sampling protocol used in these studies, we acknowledge that our sample
299 size, n=56 at the Greenland Sea ice margin, is not ideal, but exceeds the statistical minimum.
300 Furthermore, the number of specimens analysed in this study considerably exceeds those of
301 Bednarsek et al. 2012c (n = 3 to 20) and Bednarsek et al. 2014b (n=10).

302 Our study confirms that pteropods are protected from natural dissolution by their
303 periostracum in the same way that other shelled molluscs are, and that their shells only
304 become vulnerable when the periostracal cover is breached. We now consider how these
305 patterns of dissolution relate to the life-history of *L. helicina helicina* and the likely causes of
306 periostracum damage and subsequent shell dissolution in their natural environment.

307

308 **Population dynamics**

309 Since shell damage and dissolution were only observed in the juvenile specimens of *L.*
310 *helicina helicina* we first of all consider the life stages represented by the two cohorts. Two
311 modal peaks in maximum shell diameter, 200 μm and 1380 μm , were observed within *L.*
312 *helicina helicina* collected at the Greenland Sea ice margin. We consider the smaller, ciliated
313 specimens to represent veligers of the 2012 recruitment (Fig. 2, V1-2), likely spawned in the
314 spring, and the larger winged specimens to represent juveniles that overwintered from the
315 2011 recruitment (Fig. 2, J1-J6), fitting the ontogenetic-size classifications of Lalli & Wells
316 (1978).

317 **Shell growth and protection.**

318 Although it is very thin, our results indicate that the pteropod periostracum, when intact,
319 protects the underlying aragonite from dissolution by shielding it from exposure to sea water.
320 However, should the periostracum of a pteropod become perforated, the shell beneath will
321 become exposed and susceptible to dissolution if the environment is undersaturated with
322 respect to carbonate. This scenario is evidenced by our observations following the 4 day
323 incubation of shells that were pristine prior to incubation. At the end of the incubation, 50 %
324 of the specimens incubated at $\Omega_{\text{Ar}} < 1$ exhibited surface scarring under light microscope (Fig.
325 9 b, c) that was localised exclusively to obvious scratch-like marking. All specimens
326 incubated within ambient waters appeared pristine (Fig. 9a). The absence of scratches on any
327 of the specimens incubated within ambient waters ($\Omega_{\text{Ar}} = 1.32$) indicates that either none of

328 the specimens in this treatment received scratches during collection, or they were scratched
329 but no dissolution occurred since the water was oversaturated with respect to aragonite. We
330 consider it unlikely that none of the 5 specimens incubated in ambient waters received any
331 superficial damage to their periostracum and therefore conclude that our incubation results
332 indicate that dissolution of the shell will only be observed under the following circumstances.
333 Firstly, dissolution will only occur localised to sites where the protective seal of the
334 periostracum is broken and aragonite and waters are in direct contact. Secondly, exposed
335 aragonite will only dissolve, and allow the scarring to become visible, when the shell is
336 exposed to undersaturated waters. Damage to the periostracum and exposure to
337 undersaturated waters are both necessary for shell dissolution in *L. helicina helicina* to occur.

338 Considering these two contributing factors we now consider our observations of living
339 specimens of *L. helicina helicina* recovered from the Greenland Sea ice margin in the context
340 of 1. how the periostracum may have become damaged and 2. where and when the juvenile
341 specimens became exposed to undersaturated waters.

342 **Damage to the periostracum**

343 Looking first at all at the pattern and distribution of dissolution exhibited on shells of *L.*
344 *helicina helicina* we consider the following hypotheses for how the perisotracum may have
345 become compromised.

346 **(i) Central whorl damage**

347 The periostracum of the initial whorl/protoconch appears to have been particularly
348 susceptible to damage. The pitted texture observed in the centre of J3-6 does not exhibit any
349 particular pattern indicative of mechanical damage. Being the oldest part of shell, it has been
350 exposed to abrasion and/or microbial erosion for the longest time and is therefore more prone
351 to loss or damage. It is also worth noting that although the mineralogy of *Limacina*
352 protoconchs have not been studied, those of some other gastropods have been shown to
353 include Amorphous Calcium Carbonate (Auzoux-Bordenave et al. 2010; Auzoux-Bordenave
354 et al. 2015) which is more unstable than aragonite and may be particularly prone to
355 dissolution. Mussel shells grown within waters of pH = 7.2 also exhibited a similar pattern of
356 shell damage whereby dissolution only occurred where the periostracum at the umbo, the

357 oldest part of the shell, had been abraded owing to adjacent mussels rubbing together
358 (Rodolpho-Metalpa et al., 2011).

359 **(i) Deep damage**

360 Exposure of multiple layers of aragonite crystals appears within the 2nd and 3rd whorls of
361 specimens J5 and J6. The original cause of the breach to the periostracum may be mechanical
362 or through erosion of the periostracum by epibiont activity. However, in the case of J6, linear
363 features to the areas of deep damage suggest a mechanical origin.

364 While the animal can generate aragonite internally to patch up areas of shell damage
365 (McMahon and Bogan, 2001), it cannot repair damage to the periostracum (Saleuddin & Petit
366 1983) and the exposed aragonite beneath will always be susceptible to dissolution if Ω_{Ar} falls
367 below 1. The exposure of multiple layers of aragonite, exceeding the thickness of the original
368 shell, suggests that the animals repaired their shells internally by patching up areas of deep
369 damage with new aragonite secreted on the inner wall of the shell. Again, since the pteropod
370 is unable to replace the periostracum and protect the newly precipitated aragonite, this area of
371 repair will continue to be dissolved from the outside so long as it is exposed to undersaturated
372 waters. In this way the areas of deep damage we observe can significantly exceed the
373 thickness of the original shell. Internal repair of this type is frequently observed in other
374 molluscs, such as Harper et al. (2012). Knowing the linear extension rate of *L. helicina*
375 *helicina* would allow the depth of the moulding of the subsequent whorls around deep
376 damage of an inner whorl to determine the rate of dissolution of the exposed shell.

377

378 **(ii) Fracture zones**

379 Only 2% of the sub-Antarctic population of *L. helicina antarctica* survive the first year
380 (Bednarsek et al., 2012c), presumably, largely due to predation. While larger predators such
381 as fish will eat the entire animal, a principal predator of *L. helicina*, is the non-shelled
382 (gymnosomatus) pteropod *Clione limacina*, which will attach itself to the prey's shell and
383 extract the animal from within (Lalli & Gilmer, 1989). In a bid to protect itself, *L. helicina*
384 will retract within its shell but, in doing so, risks damage to the most newly formed, outer
385 edge of its shell during failed predation attempts. The distinctive fracture zones reported here
386 are indicative of the shell aperture having been broken at some point in the past and

387 subsequently repaired and are similar to failed predation scars found on other gastropods
388 (Alexander & Dietl, 2003). Scratch-like markings perpendicular to the fracture line,
389 frequently observed on specimens recovered from the Greenland Sea ice margin (Fig 10) may
390 indicate *C. limacina* predation attempts. The damage caused to *L. helicina* during such
391 predation attempts appears to be readily recoverable and subsequent regrowth of new
392 ‘pristine’ shell from broken apertures is commonly observed (Fig. 5, 7, 8, 10; Lischka &
393 Riebesell, 2012; Comeau et al., 2012; Bednarsek et al., 2012a [supplementary Fig. 2]). While
394 in the ciliated, veliger stage, the animal is less agile and it is likely that predation attempts at
395 this stage are highly successful which explains why none of the veligers showed failed
396 predation damage. Animals that survive this first season to become fully-winged juveniles
397 become better able to evade predation attempts. What is unique to the specimens collected in
398 the Greenland Sea ice margin is frequent occurrence of dissolution localised to fractures and
399 surface damage. The suture between the damaged shell and regrowth appears to be
400 particularly prone to dissolution. SEM images (Fig. 7 and 8) suggest that the incomplete
401 merger of old fractured periostracum and new periostracum grown at the aperture edge may
402 allow a thin band of aragonite to become exposed and dissolved in when undersaturated
403 waters, which can undermine the periostracum adjacent to the breach. Animals that survive
404 the first year will carry the scars of predatory damage into later life.

405 **Exposure to understaturated waters**

406 At the time of collection, the entire depth of the water column at the Greenland Sea ice
407 margin was over-saturated with respect to aragonite (Fig. 2). At these Ω_{Ar} values we would
408 not expect to observe any signs of shell dissolution, as is the case at the open water sites in
409 the Greenland and Barents Sea and the pristine specimens incubated in ambient waters from
410 the Greenland Sea ice margin. Furthermore, the absence of any damage observed on the
411 veligers, which were likely to have been spawned just weeks earlier, is consistent with them
412 growing in supersaturated waters. However, the high incidence of shell damage to the 2011
413 recruitment suggests that these specimens had been exposed to lower Ω_{Ar} at some point
414 within the last year. In April 2010, Comeau et al. (2012) collected *L. helicina helicina* below
415 first year sea ice in the Canadian Arctic. In this ~350 m water depth shelf setting, specimens
416 were recovered from the upper 200 m of the water column where Ω_{Ar} was found to vary
417 between 1.07 and 1.40. These Ω_{Ar} values are similar to measurements collected beneath sea
418 ice in the Amundsen Gulf, Arctic Sea, in April 2008 (Fransson et al., 2013). Fransson et al.

419 (2013) observed the lowest Ω_{Ar} beneath Arctic sea ice water during April following the
420 accumulation of CO₂-enriched brines expelled into sub-sea ice waters during sea ice
421 formation through the winter months in addition to CO₂ produced by the remineralisation of
422 organic matter beneath the sea ice (Chierici et al., 2011). By May, the release of CO₂-
423 depleted melt water and the onset of photosynthesis reduced dissolved CO₂ concentrations in
424 the mixed layer waters, thus increasing [CO₃²⁻] and pH and seeing Ω_{Ar} reaching values of up
425 to 2 (Fransson et al., 2013). Assuming similar processes control under sea ice waters within
426 the Greenland Sea, we anticipate that Ω_{Ar} would have been lower during the winter months of
427 2011/2012 than observed in June 2012 when sea ice melt was underway and phytoplankton
428 production was well established. We illustrate our proposed life history, including failed
429 predation, shell repair and regrowth and subsequent dissolution in undersaturated waters over
430 winter in Figure 11.

431 **Dead animal shell dissolution**

432 We observed that the shells of dead specimens dissolved uniformly (cf. Gerdherdt & Henrich,
433 2001). We propose that the shells of dead specimens, with a fully intact periostracum,
434 dissolve from the inside (cf. Tunnicliffe et al., 2009). Degradation of the animal's body
435 would lower the saturation state internally, so regardless of the saturation state of the
436 surrounding water, the shell is vulnerable to dissolution once the animal is dead. This may
437 account for the sparse occurrence of pteropods within seafloor sediments, even those above
438 the lysocline (Hunt et al., 2008).

439 **Effect of dissolution on animal health**

440 Regrowth and internal repair of the shell demonstrates the ability of *L. helicina helicina* to
441 maintain shell integrity following trauma. In fact the animals that exhibited extensive areas of
442 deep dissolution were not markedly smaller than those with pristine shells. However, energy
443 required to repair the shell from the inside may have a somatic or reproductive cost. This is
444 seen in other species of mollusc exposed to elevated *p*CO₂ conditions (Wood et al., 2008;
445 2010)

446 **Removal of periostracum prior to visual inspection**

447 Our observation of discrete regions of shell dissolution, localised to areas of periostracum
448 damage is consistent with observations on larger mollusc shells (Tunnicliffe et al., 2009;

449 Rodolfa-Metalpa et al., 2011; Garilli et al., 2015), but contrary to the findings of Bednarsek et
450 al. (2012a) who report dissolution over the entirety of *L. helicina antarctica* shells in a region
451 of upwelling in the Southern Ocean. Bednarsek et al. (2012a) noted that the dissolution
452 response they report is similar to that of dead animals incubated at $\Omega_{Ar}=1$ (Byrne et al., 1984;
453 Feely et al., 1988) and claimed that this was evidence that pteropods ‘have little to protect
454 themselves from Ω_{Ar} under-saturation’. Our study, however, raises concerns about the
455 preparation methods used in studies of live-collected material. As previously demonstrated by
456 Lischka et al. (2011), Lischka & Riebesell (2012a), and Comeau et al. (2012), we show that
457 dissolution of pteropod shells is readily evident under light microscope. The use of SEM
458 images provides context to the nature and pattern of the dissolution. Bednarsek et al. (2012a)
459 do not provide any light microscope images and use an extensive method to prepare
460 specimens for SEM analysis (detailed in Bednarsek et al., 2012b) meaning it has not been
461 possible to directly compare our observations. Furthermore, since these are two subspecies,
462 identical treatment of samples would be necessary to ensure any species-specific responses
463 are accurately observed. We therefore highlight the need for uniformity of approach, also for
464 techniques to be employed that do not involve chemical reaction or plasma etching with the
465 outer shell layers. Wholesale removal of the periostracum inhibits recognition between
466 dissolution which has occurred to the living specimen due to natural damage to the
467 periostracum, as opposed to ‘bleaching’ of shells prior to analysis which can cause post-
468 mortem damage to the crystalline fabric of the shells. The latter is particularly important as it
469 is well known that shell microstructures contain both inter and intracrystalline organic matrix
470 (Marin et al 1996), the selective removal of which may produce a corroded appearance (see
471 Peck et al., 2015) which may be misinterpreted. We encourage the development of protocols
472 that allow for dissolution to be documented and quantified using minimal preparation, in
473 particular avoiding chemical treatment of the shell surface.

474 **Conclusions**

475 For molluscs (Tunnicliffe et al., 2009) and other genera (Rodolfo-Metalpa. et al., 2011; Ries
476 et al., 2009) living in under-saturated waters, the periostracum, an organic external layer
477 provides a vital means of protecting the shells and exoskeletons from dissolution and
478 therefore ensuring the vitality of the animal. The effectiveness of the periostracum to
479 pteropods however has been brought into question in recent years (Bednarsek et al., 2012a;
480 Bednarsek et al., 2014a). We demonstrate that, in *L. helicina helicina*, shell dissolution can

481 occur where the periostracum has been breached. Where the periostracum has remained intact
482 however, the shell appears pristine with no sign of dissolution, even when exposed to $\Omega_{Ar} \leq 1$.
483 Since the periostracum appears to offer such effective protection of the shell we propose that
484 the extent of shell dissolution is not a direct function of exposure to undersaturated waters,
485 rather it is dependent on the extent of periostracal damage and exposure to undersaturated
486 waters. In addition to being able to protect their shells from whole scale dissolution, where
487 localised dissolution has occurred due to trauma to the periostracum the shell may become
488 thicker than the original shell, indicating that the animal is able to secrete layers of aragonite
489 internally to patch up localised damage. Furthermore, our observations support rinsing and
490 drying specimens on collection to enable shell damage to be identified with light microscopy
491 (Lischka et al., 2011), and we caution against the use of chemical or laser etching of the
492 periostracum before visual analysis.

493 While we propose that *L. helicina helicina* are perhaps not as vulnerable to ocean
494 acidification as previously claimed, at least not from direct shell dissolution, we have not
495 assessed the energetic consequences of calcifying a shell in under saturated waters and
496 repairing and maintaining a damaged shell within waters of $\Omega_{Ar} \leq 1$. Further investigation into
497 the long term reproductive and somatic consequences of ocean acidification are needed.

498

499 **Acknowledgements**

500 We thank the captains and crew of the RRS *James Clark Ross* for enabling this research to be
501 carried out, and PSO Ray Leaky. We are grateful for funding support from NERC, Defra and
502 DECC to the pelagic consortium of the UK Ocean Acidification programme (grant no.
503 NE/H017348/1*). Thank you to Alex Ball and Tomasz Goral at the Natural History Museum
504 for assisting with SEM imaging.

505

506 **References**

507 Alexander, R. & Dietl, G. 2003. The fossil record of shell-breaking predation on marine bivalves
508 and gastropods, in 'Predator Prey Interactions in the Fossil Record', Springer, pp. 141–
509 176.

510 Auzoux-Bordenave, S., Badou, A., Gaume, B., et al. 2010. Ultrastructure, chemistry and
511 mineralogy of the growing shell of the European abalone *Haliotis tuberculata*. *Journal of*
512 *Structural biology* 171, 277-290.

513 Auzoux-Bordenave S, Brahmi C, Badou A, et al. 2015. Shell growth, microstructure and
514 composition over the development cycle of the European abalone *Haliotis tuberculata*.
515 *Marine Biology* 162, 687-697.

516 Bandel, K.1990. Shell structure of the gastropoda excluding archaegastropoda. In: Carter, J.G.
517 (Ed.), *Skeletal Biomineralization: Patterns, Processes, and Evolutionary Trends*, Vol. 1.
518 Van Nostrand Reinhold, New York, pp. 1-832.

519 Bednaršek, N., Tarling, G.A., Bakker, D.C.E., et al. 2014a. Dissolution dominating calcification
520 process in polar pteropods close to the point of aragonite undersaturation. *PLoS ONE*,
521 9(10), e109183, doi: 10.1371/journal.pone.0109183.

522 Bednaršek, N., Feely, R.A., Reum, J.C.P., et al. 2014b. *Limacina helicina* shell dissolution as an
523 indicator of declining habitat suitability due to ocean acidification in the California
524 Current Ecosystem. *Proc. Roy. Soc. B*, 281, 20140123, doi: 10.1098/rspb.2014.0123.

525 Bednaršek, N., et al., 2012a. Description and quantification of pteropod shell dissolution: a
526 sensitive bioindicator of ocean acidification. *Glob. Change Biol.* 18, 2378–2388.
527 doi:10.1111/j.1365-2486.2012.02668.x)

528 Bednaršek, N., et al., 2012b, Population dynamics and biogeochemical significance of *Limacina*
529 *helicina antarctica* in the Scotia Sea (Southern Ocean). *Deep-Sea Research II*, 59-60,
530 105–116.

531 Bednaršek, N., et al. 2012c. Extensive dissolution of live pteropods in the Southern Ocean. *Nat.*
532 *Geosci.* 5, 881–885. doi:10.1038/ngeo1635.

533 Bednaršek, N., Možina, J., Vogt, M., et al., 2012d. The global distribution of pteropods and their
534 contribution to carbonate and carbon biomass in the modern ocean. *Earth Syst. Sci. Data*,
535 4, 167–186, doi: 10.5194/essd-4-167-2012.

536 Byrne, R.H., J.G. Acker, P.R. Betzer, R.A. Feely, and M.H. Cates. 1984. Water column
537 dissolution of aragonite in the Pacific Ocean. *Nature*, 312, 321–326

538 Caldeira, K. & Wickett, M.E. 2003. Anthropogenic carbon and ocean pH. *Nature* 425, 365.

539 Chierici, M., Fransson, A. Lansard, B., et al. 2011. The impact of biogeochemical processes and
540 environmental factors on the calcium carbonate saturation state in the circumpolar flow

541 lead in the Amundsen Gulf, Arctic Ocean. *J. Geophys. Res.*, 116, C00G09,
542 doi:10.1029/2011JC007184.

543 Comeau S, Alliouane S, Gattuso JP. 2012. Effects of ocean acidification on overwintering
544 juvenile Arctic pteropods *Limacina helicina*. *Marine Ecology Progress Series* 456: 279–
545 284. doi: 10.3354/meps09696

546 Comeau, S., Gorsky, G., Jeffree, R., et al. 2009. Impact of ocean acidification on a key Arctic
547 pelagic mollusc (*Limacina helicina*). *Biogeosciences*, 6 (9): 1877. doi:10.5194/bg-6-
548 1877-2009.

549 Comeau S, Jeffree R, Teyssié JL, Gattuso JP. 2010. Response of the Arctic pteropod *Limacina*
550 *helicina* to projected future environmental conditions. *PLoS ONE* 5:e11362

551 Dickson, A. G. & Millero, F. J. 1987. A comparison of the equilibrium constants for the
552 dissociation of carbonic acid in seawater media. *Deep-Sea Res Part A*, 34, 1733–1743.

553 Dickson AG, Sabine CL, Christian JR (eds). 2007. Guide to best practices for CO₂
554 measurements. PICES Special Publication 3, PICES, Sidney, BC

555 Fabry, V.J., J.B. McClintock, J.T. Mathis, & J.M. Grebmeier. 2009. Ocean acidification at high
556 latitudes: The bellwether. *Oceanography* 22(4), 60–171

557 Feely, R.A. et al. 1988. Winter-summer variations of calcite and aragonite saturation in the
558 northeast Pacific. *Mar. Chem.*, 25, 227–241

559 Fransson, A., Chierici, M., Miller, L.A., et al. 2013. Impact Of Sea-Ice Processes On The
560 Carbonate System And Ocean Acidification At The Ice-Water Interface Of The
561 Amundsen Gulf, Arctic Ocean. *Journal of Geophysical Research: Oceans*, 1, pp.1-81

562 Gannefors, C., Böer, M., Kattner, G., et al. 2005. The Arctic sea butterfly *Limacina helicina*:
563 Lipids and life strategy. *Marine Biology*, 147, 169. doi:10.1007/s00227-004-1544-y.

564 Garilli, V., Rodolfo-Metalpa, R., Scuderi, D., et al. 2015. Physiological advantages of dwarfing
565 in surviving extinctions in high-CO₂ oceans. *Nature Climate Change*,
566 doi:10.1038/NCLIMATE2616

567 Gattuso JP, Gao K, Lee K, Rost B, and Schulz KG. 2010. Approaches and tools to manipulate
568 the carbonate chemistry. In: Riebesell U, Fabry VJ, Hansson L, Gattuso JP (eds) Guide to
569 best practices for ocean acidification research and data reporting. Publications Office of
570 the European Union, Luxembourg, p 243–258

571 Gerhardt, S. & Henrich, R. 2001. Shell preservation of *Limacina inflata* (Pteropoda) in surface
572 sediments from the Central and South Atlantic Ocean: a new proxy to determine the
573 aragonite saturation state of water masses, *Deep-Sea Res. I*, 48, 2051–2071.

574Harper, E. M. 1997. The molluscan periostracum: an important constraint in bivalve evolution.
575 *Palaeontology*, 40, 71–97.

576Harper, E.M., Clark, M.S., Hoffman, J. I et al. 2012. Iceberg scour and shell damage in the
577 Antarctic bivalve *Laternula elliptica*. *PLoS One* , 7 (9). e46341

578Hunt B., et al., 2008. Pteropods in Southern Ocean ecosystems. *Progress in Oceanography*, 78,
579 193–221.

580Hunt, B., Strugnell, J., Bednarsek, N., et al. 2010. Poles apart: the “bipolar” pteropod species
581 *Limacina helicina* is genetically distinct between the Arctic and Antarctic oceans *Plos*
582 *One* e9835.

583Lalli, C.M., & Gilmer R.W. 1989. Pelagic Snails: The Biology of Holoplanktonic Gastropod
584 Mollusks, Stanford University Press, Stanford, CA, USA.

585Lalli, C.M. & Wells, F.E., 1978. Reproduction in the genus *Limacina* (Opisthobranchia:
586 Thecosomata). *Journal of Zoology (London)* 186, 95–108.

587Lewis E, & Wallace DWR. 1998. Program developed for CO2 system calculations. Technical
588 Report ORNL/CDIAC-105. Carbon Dioxide Information Analysis Center, Oak Ridge
589 National Laboratory, USDepartment of Energy, Oak Ridge, TN, USA.

590Lischka S, Büdenbender J, Boxhammer T, Riebesell U. 2012. Impact of ocean acidification and
591 elevated temperatures on early juveniles of the polar shelled pteropod *Limacina helicina*:
592 mortality, shell degradation, and shell growth. *Biogeosciences*, 8, 919–932.

593Lischka, S. &Riebesell U. 2012 Synergistic effects of ocean acidification and warming on
594 overwintering pteropods in the Arctic. *Glob. Change Biol.* 18, 3517–3528. doi:10.1111/
595 gcb.12020)

596Lischka S, Budenbender J, Boxhammer T, Riebesell U. 2011. Impact of ocean acidification and
597 elevated temperatures on early juveniles of the polar shelled pteropod *Limacina helicina*:
598 mortality, shell degradation, and shell growth. *Biogeosciences* 8: 919–932. doi:
599 10.5194/bg-8-919-2011.

600Marin, F., Smith, M., Isa, Y., Muyzer, G., Westbroek, P. 1996. Skeletal Matrices, mucin, and the
601 origin of invertebrate calcification. *Proceedings of the National Academy of Sciences of*
602 *the United States of America* 93 1554-1559

603McMahon R.F. & Bogan A.E. 2001. - Ecology and classification of North American freshwater
604 invertebrates. Pages 331-429 in *Mollusca: Bivalvia* (2nd edition). Thorp J.H. & Covich
605 A.P. (eds). Academic Press, San Diego

606McNeil B. I., & Matear R. J. 2008. Southern Ocean acidification: A tipping point at 450-ppm
607 atmospheric CO₂. *Proc Natl Acad Sci USA*, 105, 18860–18864.

608Mehrbach, C., Ch. Culberso, J.E. Hawley, and Rm. Pytkowic. 1973. Measurement of apparent
609 dissociation constants of carbonic acid in seawater at atmospheric pressure. *Limnol.*
610 *Oceanogr.* 18, 897–907.

611Mucci, A. 1983. The solubility of calcite and aragonite in seawater at various salinities,
612 temperatures and one atmosphere total pressure. *Am. J. Sci.* 28, 780-799.

613Orr J.C., Fabry, Aumont, V.J. et al. 2005. Anthropogenic ocean acidification over the twenty-first
614 century and its impact on calcifying organisms. *Nature*, 437: doi: 10.1038/nature04095

615Peck, L. S., Clark, M., Power, D., et al. 2015 Acidification effects on biofouling communities:
616 winners and losers. *Global Change Biology*, doi: 10.1111/gcb.12841

617Pierrot, D. E. L. & Wallace, D. W. R. 2006. MS Excel program developed for CO₂ System
618 Calculations. ORNL/CDIAC-105, Oak Ridge, Tennessee, Carbon Dioxide Information
619 Analysis Center, Oak Ridge National Laboratory, US Department of Energy.

620Ries J.B., Cohen, A. L., McCorkle, D. C. 2009. Marine calcifiers exhibit mixed responses to
621 CO₂-induced ocean acidification. *Geology*, 37, 1131–1134.

622Rodolfo-Metalpa, R., Houlbreque, F., Tambutte, E., et al. 2011. Coral and mollusk resistance to
623 ocean acidification adversely affected by warming. *Nature Climate Change*, 1, 308–312.

624Sabine, C. L., Feely, R. A., Gruber, N., et al. 2004. The Oceanic Sink for Anthropogenic CO₂.
625 *Science*, 305, 367-371.

626Saleuddin, A. S. M., & Petit, H.P. 1983. The mode of formation and the structure of the
627 periostracum. In: Saleuddin ASM, Wilbur KM editors. *The Mollusca*. Vol. 4: Physiology
628 Part I. New York: Academic Press. 199–234.

629Sato-Okoshi W, Okoshi K, Sasaki H, Akiha F., 2010. Shell structure characteristics of pelagic
630 and benthic molluscs from Antarctic waters. *Polar Science*, 4, 257–261.

631Taylor, J. D., and Kennedy, W. J. 1969. The influence of the periostracum on the shell structure
632 of bivalve molluscs. *Calc. Tiss. Res.* 3, 274–283

633Tunnicliffe, V., Davies K. T., Butterfield, D. A., Embley, R.W., Rose, J. M., and W. W.
634 Chadwick, W. W. Jr., 2009. Survival of mussels in extremely acidic waters on a
635 submarine volcano. *Nature Geosciences*, 2, 344-348. DOI: 10.1038/NGEO500

636Wood, H.L., Spicer, J.I., Widdicombe, S. 2008. Ocean acidification may increase calcification
637 rates, but at a cost. *Proceedings of the Royal Society B: Biological Sciences* 275.1644,
638 767-1773.

639 Wood, H. L., et al. 2010. Interaction of ocean acidification and temperature; the high cost of
640 survival in the brittlestar *Ophiura ophiura*. *Marine Biology*, 157, 2001-2013.

641

642 **Figure captions**

643 **Figure 1. Location of the three sites referred to in this study and sea ice coverage on**

644 **June 18th 2012.** Greenland Sea ice margin site, orange; Greenland open water site, dark blue;

645 Barents Sea site, light blue.

646 **Figure 2. Water column profiles of temperature, salinity and Ω_{Ar} at the three sites**

647 **referred to in this study.** A. Temperature, B. Salinity, C. Ω_{Ar} . Greenland Sea ice margin site,

648 orange; Greenland open water site, dark blue; Barents Sea site, light blue. Dotted line at 200

649 m indicated the depth from which the Bongo net was vertically hauled.

650 **Figure 3. Maximum shell diameter distribution of *L. helicina helicina* specimens**

651 **recovered from the Greenland Sea ice margin.** Two distinct cohorts of ciliated veligers and

652 winged juveniles were observed.

653 **Figure 4. Light microscope images of examples of *L. helicina helicina* collected at the**

654 **Greenland Sea ice margin.** V1-2 are veligers from the 2012 recruitment (scale bars 100

655 μm). J1-6 juveniles from the 2011 recruitment (scale bars 250 μm). J1-2, exhibit fully

656 translucent/pristine shells. J3-4, exhibit some areas of opaque shell, but no deep damage. J5-

657 6, exhibit areas of opaque shell with some deep damage.

658 **Figure 5. Light microscope images of examples of *L. helicina helicina* from the open**

659 **water sites in the Greenland Sea and Barents Sea exhibiting fracture and repair but no**

660 **areas of opaque shell.**

661 **Figure 6. Light microscope and SEM images of J3 (a, b, c; LEO) and J4 (d, e, f; Ultra**

662 **Plus [uncoated]).**

663 **Figure 7. Light microscope and Ultra Plus (coated) SEM images of J5.** C-E, focus on an

664 area of deep damage in the third whorl. In C and E note how the fourth whorl moulds around

665 the deep damage of the third whorl. In D note how multiple layers of aragonite have been

666 exposed and how deep damage exceeds the depth of the original shell, B. F, G and H focus

667 on a fracture in the third whorl. F shows a neat suture between old shell, below the fracture,

668 and new shell above. Moving along the fracture, G, aragonite crystals become exposed where
669 the suture between the periostracum of the old and new shell was not adequate to protect the
670 shell beneath and dissolution has occurred. The area circled in G is shown in H. A piece of
671 periostracum that has become loose as under-saturated waters have undermined the
672 periostracum from the suture and dissolved the shell from beneath it.

673 **Figure 8. Light microscope and Ultra Plus (uncoated) SEM images of J6.** C and D focus
674 on areas of deep damage in the third whorl. Note that multiple layers of aragonite are exposed
675 and how the fourth whorl moulds around the deep damage of the third whorl. E and F focus
676 on a fracture in the third whorl. Notice how the old shell, above the fracture (F) presents a
677 pitted appearance, suggesting that the periostracum and outer aragonite layer is compromised,
678 while the new shell, below the fracture, appears pristine.

679 **Figure 9. Light microscope images of pristine specimens collected from the Greenland**
680 **Sea ice margin after 4 day incubation.** A, B and C were pristine, actively swimming
681 specimens incubated at A. Ambient, B. 650 μatm target $p\text{CO}_2$ and C. 800 μatm target $p\text{CO}_2$.
682 A remained fully translucent superficial scratch marks appear after living specimens with
683 pristine shells incubated in undersaturated waters, B and C. Non-living specimens incubated
684 in ambient waters, D and at 650 μatm target $p\text{CO}_2$, E both exhibited uniform dissolution
685 across the entire shell, but the sheen of periostracum can still be seen externally, indicating
686 that the shell is dissolving internally.

687 **Figure 10. SEM images showing scratches indicative of failed predation attempts.**
688 **Scratches were observed on J4, J5 and J6, from the Greenland Sea ice margin and also**
689 **one specimen collected from the Greenland Sea open water site, D.**

690 **Figure 11. Schematic showing possible history of damage and exposure to**
691 **undersaturated waters of the 2011 recruitment, collected on June 18th 2012 as juveniles.**

692

693

694

695

696

697 **Table 1. Location and dates of sites discussed in this study.**

Date	Location	Lat	Long
18 th June 2012	Greenland Sea ice margin (sea ice)	78.16	-4.18
21 st June 2012	Greenland Sea (open water)	77.93	9.14
23 rd June 2012	Barents Sea (open water)	74.09	26.00

698

699

700 **Table 2. Incubation of pristine juvenile specimens collected within Greenland Sea ice.**

Target pCO ₂	<i>Salinity</i>	<i>TA</i>	<i>Temp</i>	<i>DIC</i>	<i>pCO₂</i>	<i>ΩAr</i>
ambient	32.59	2229.3	-1.58	2120.9	344.7	1.32
650	32.59	2241.8	-1.58	2154.7	657.4	0.76
800	32.59	2231.3	-1.58	2198.1	810.3	0.63

701

Fig. 1.

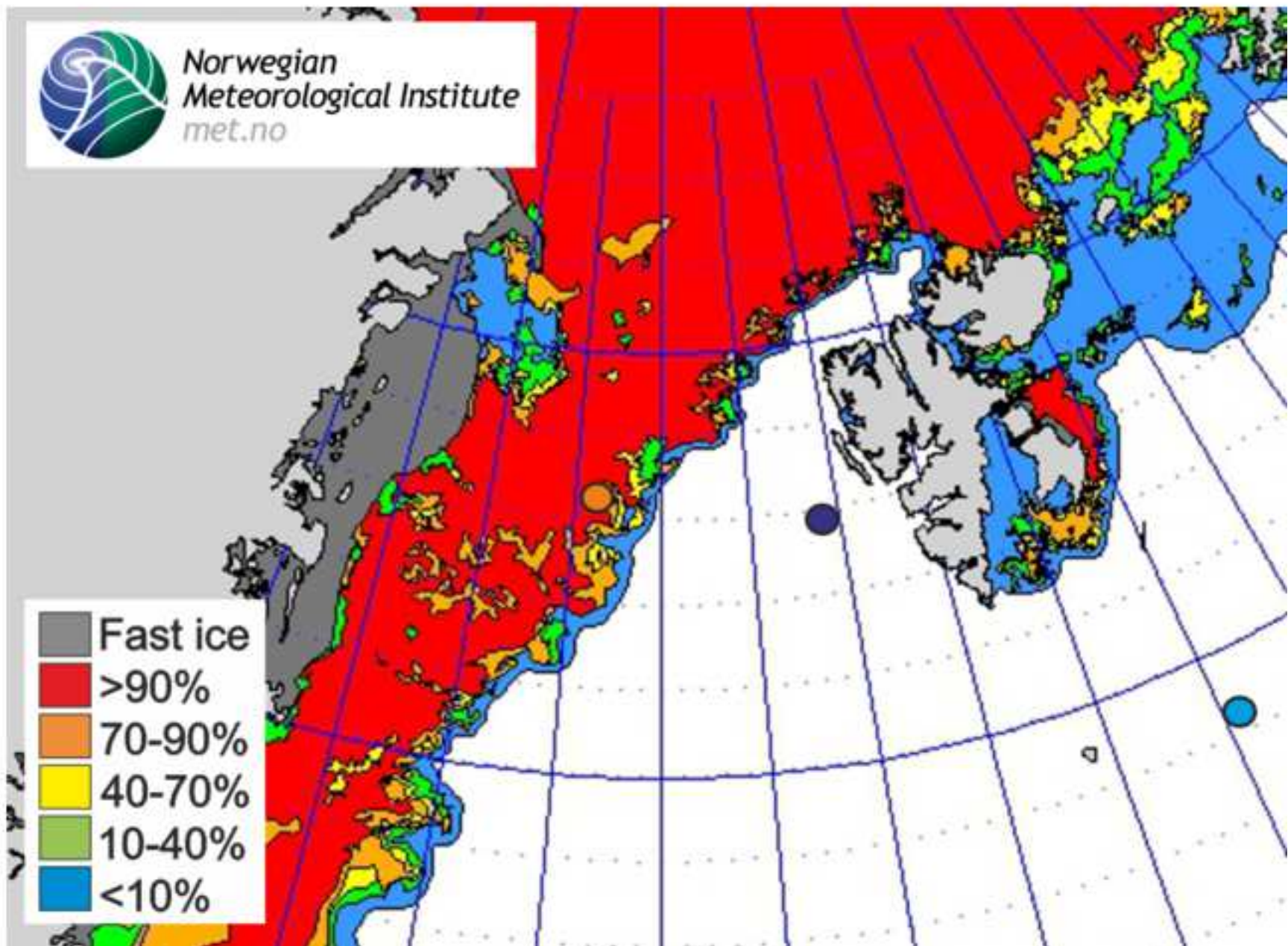


Figure 2
[Click here to download high resolution image](#)

Fig. 2

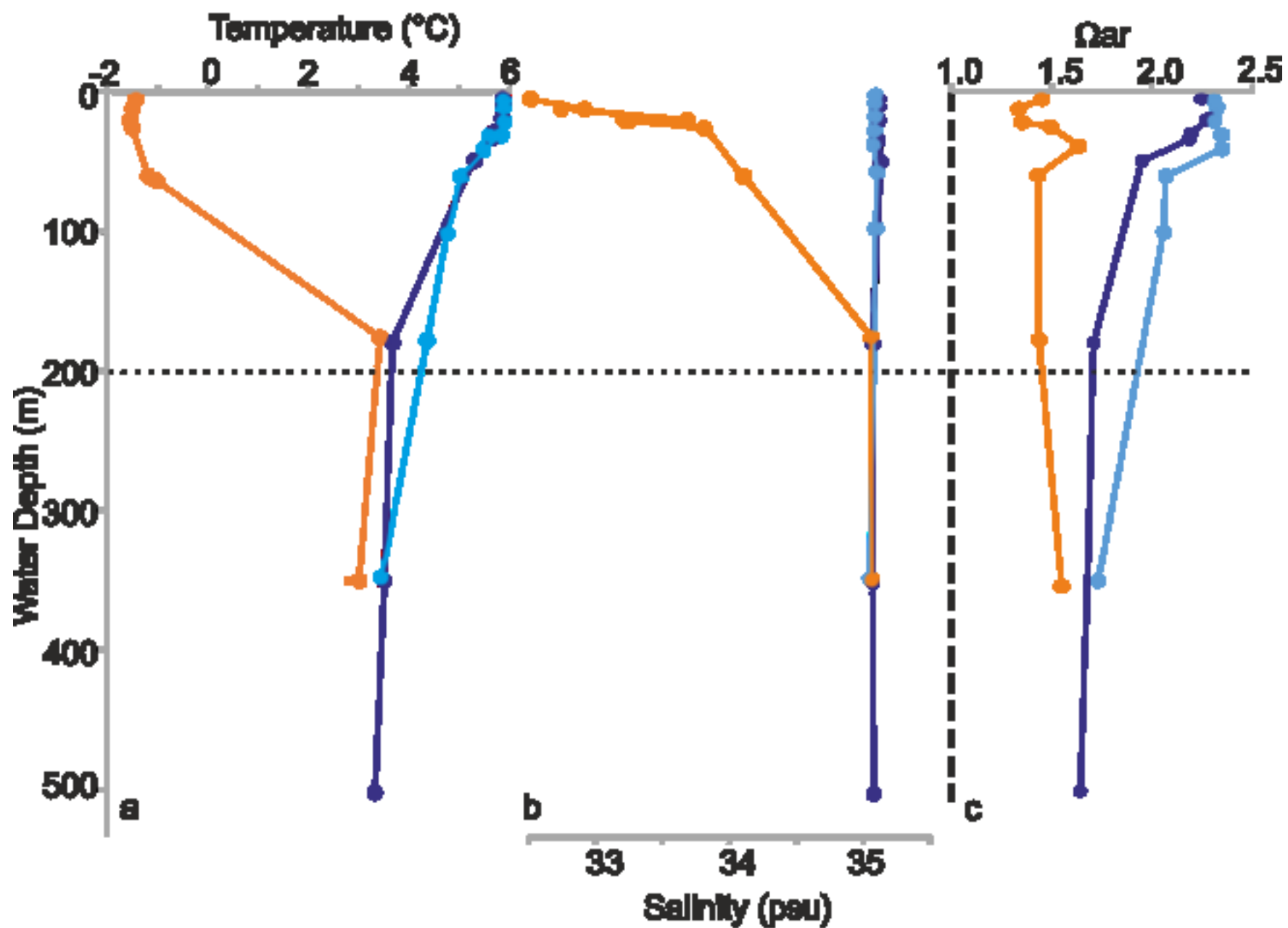


Fig 3.

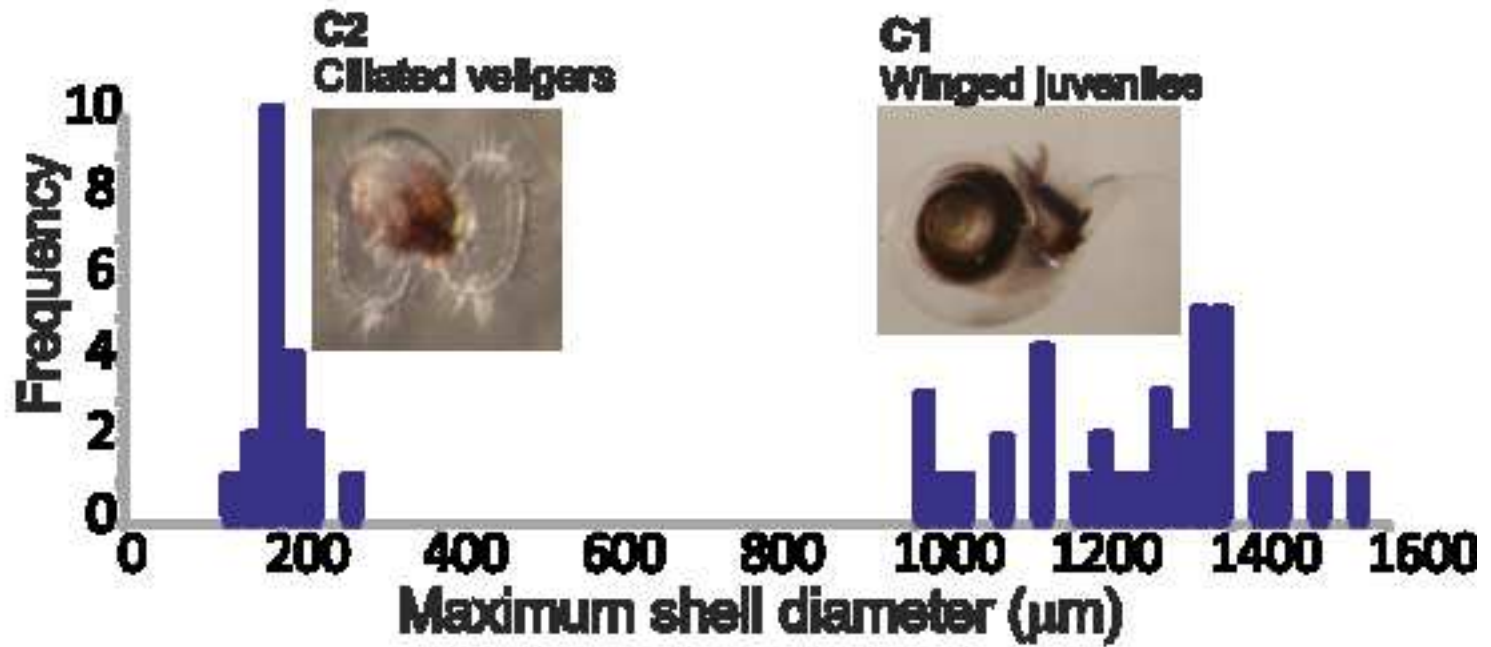


Fig. 4

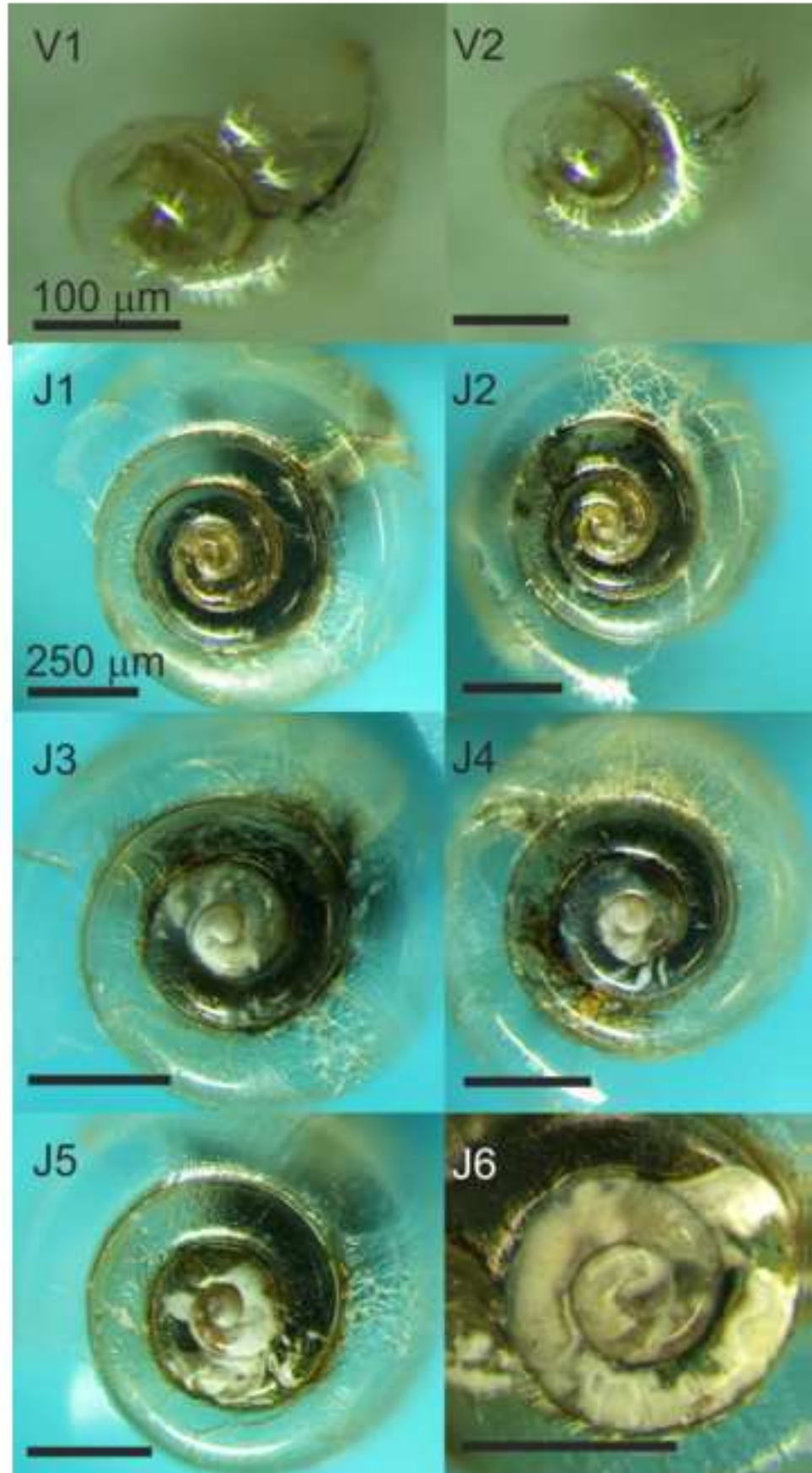


Fig. 5

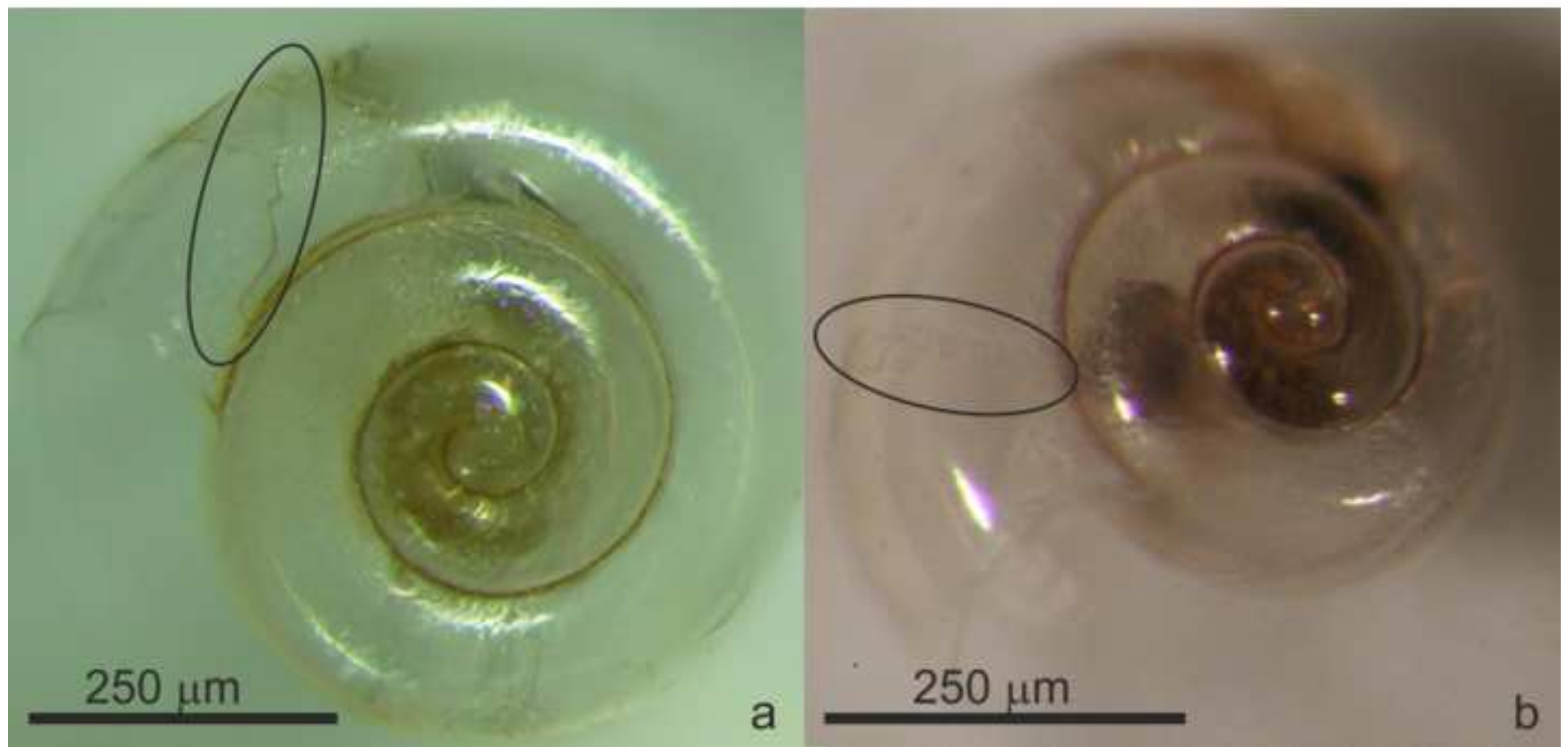


Fig 6

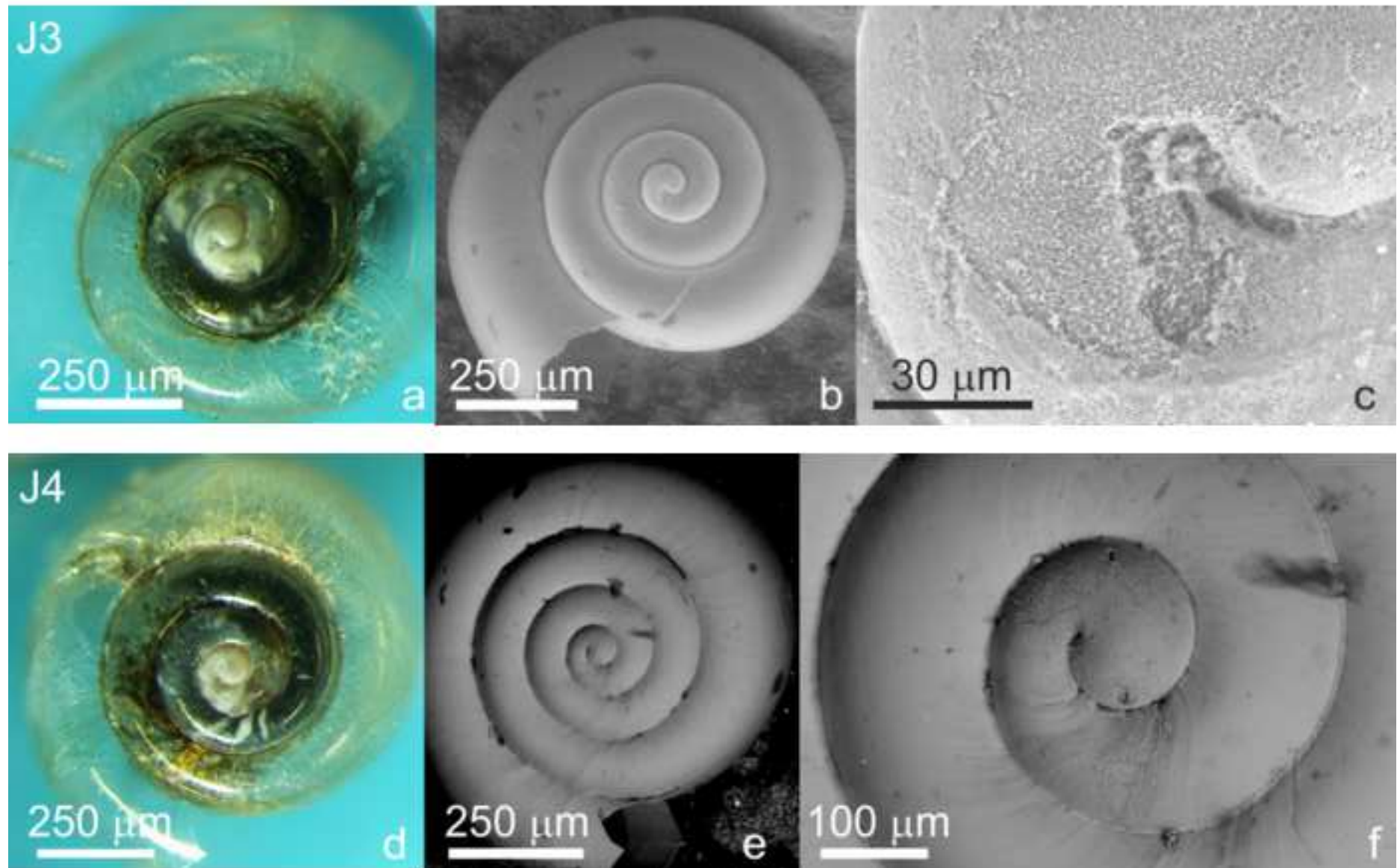


Fig 7

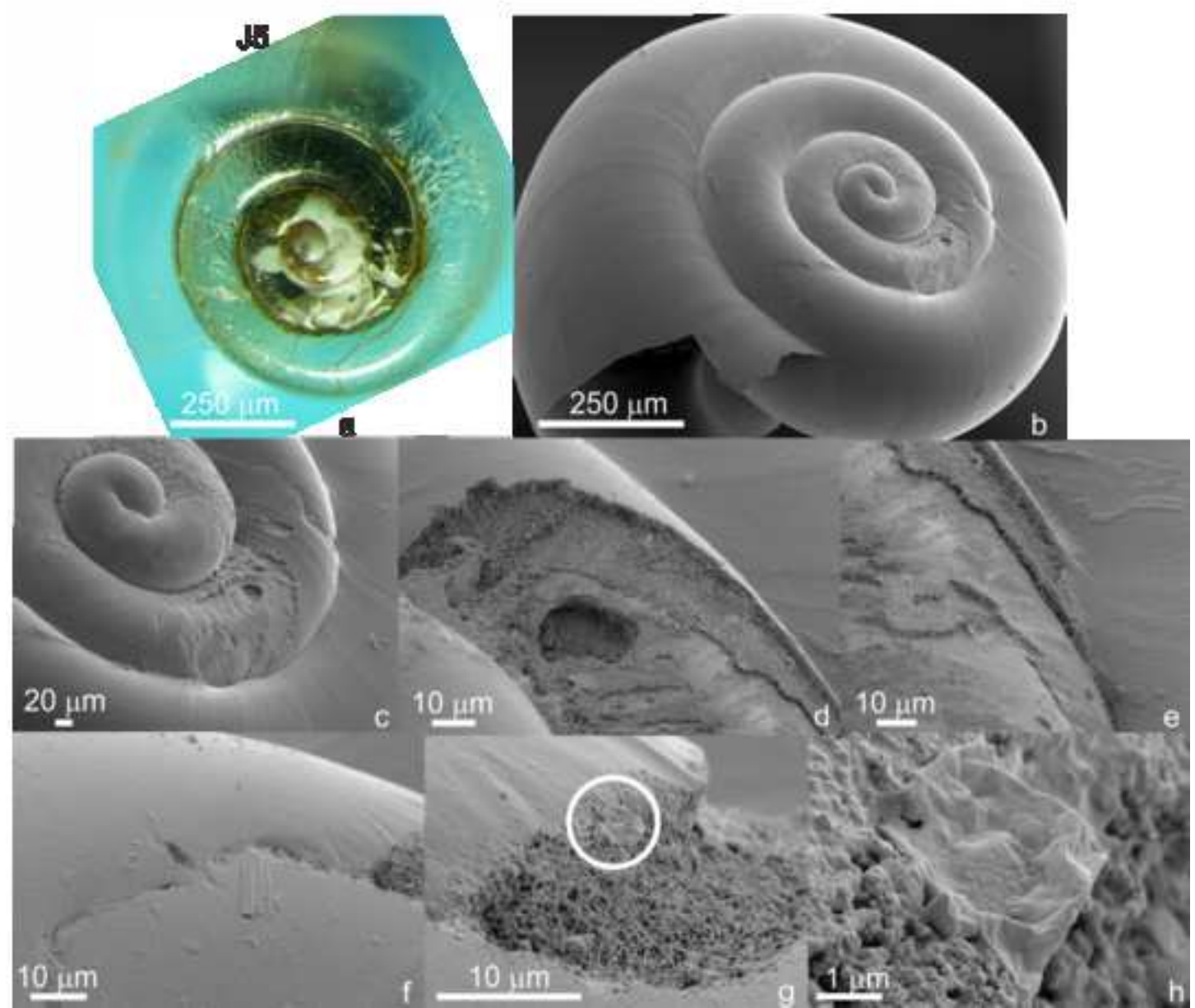


Fig 8

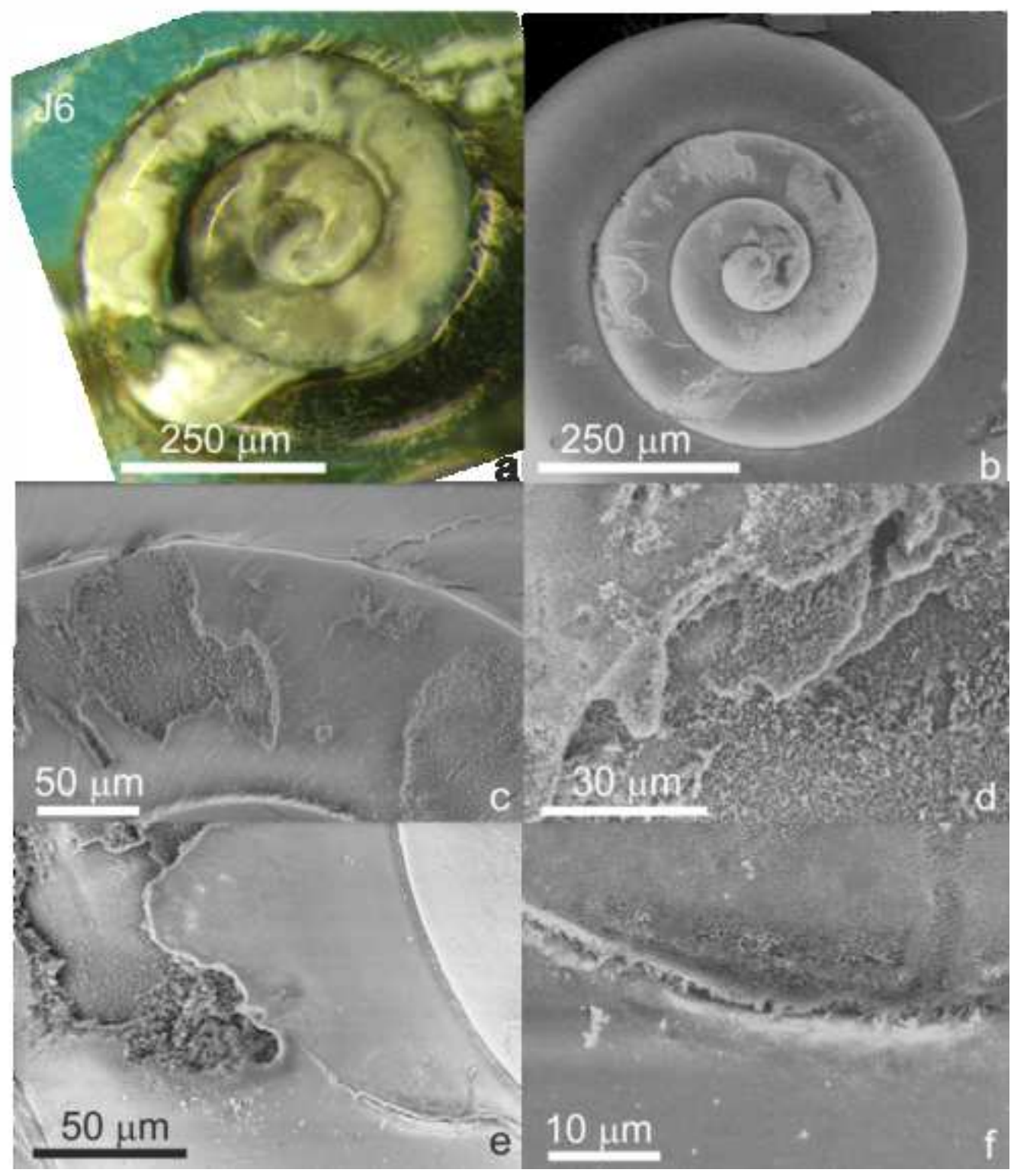


Fig 9

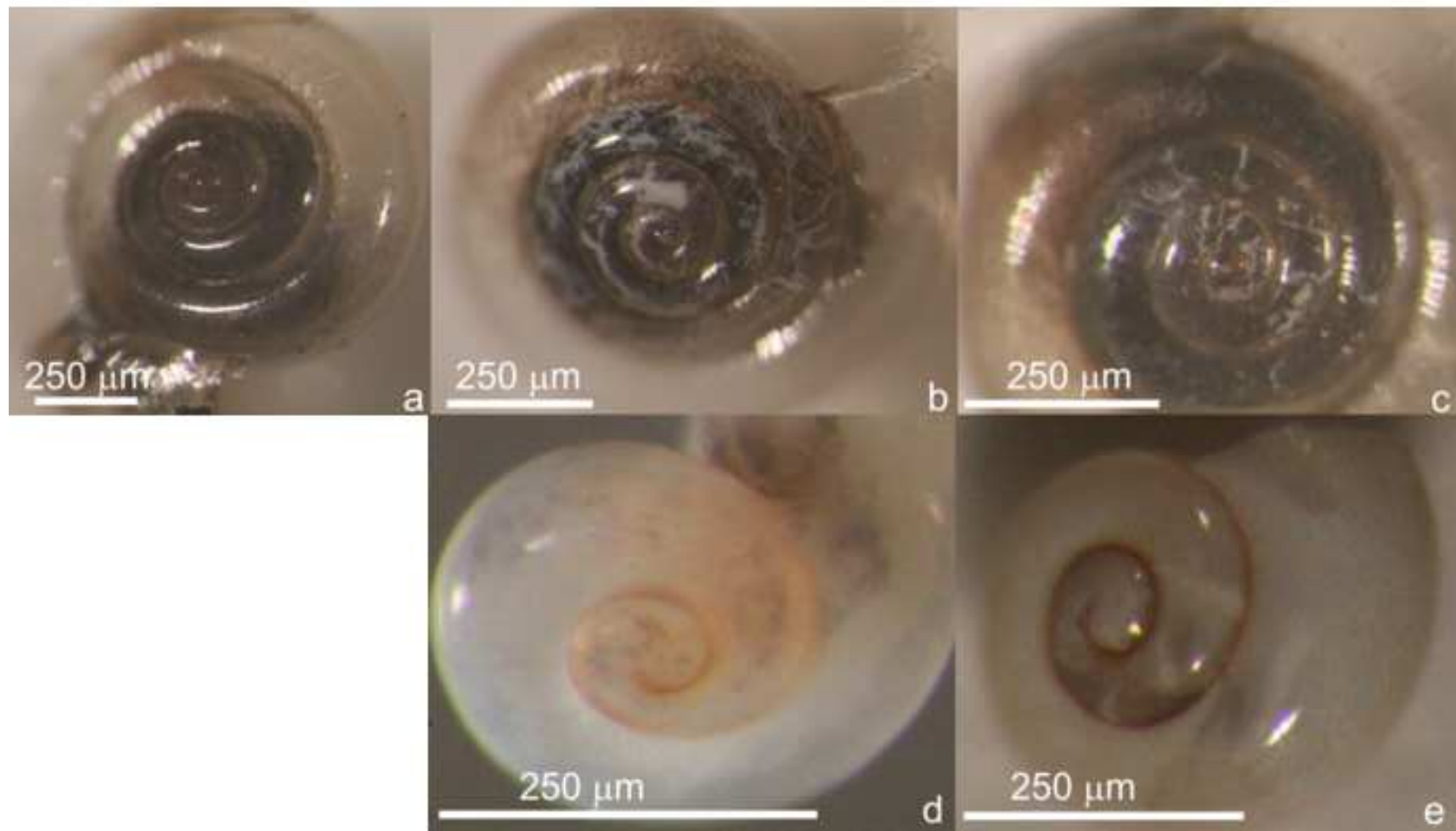


Fig 10

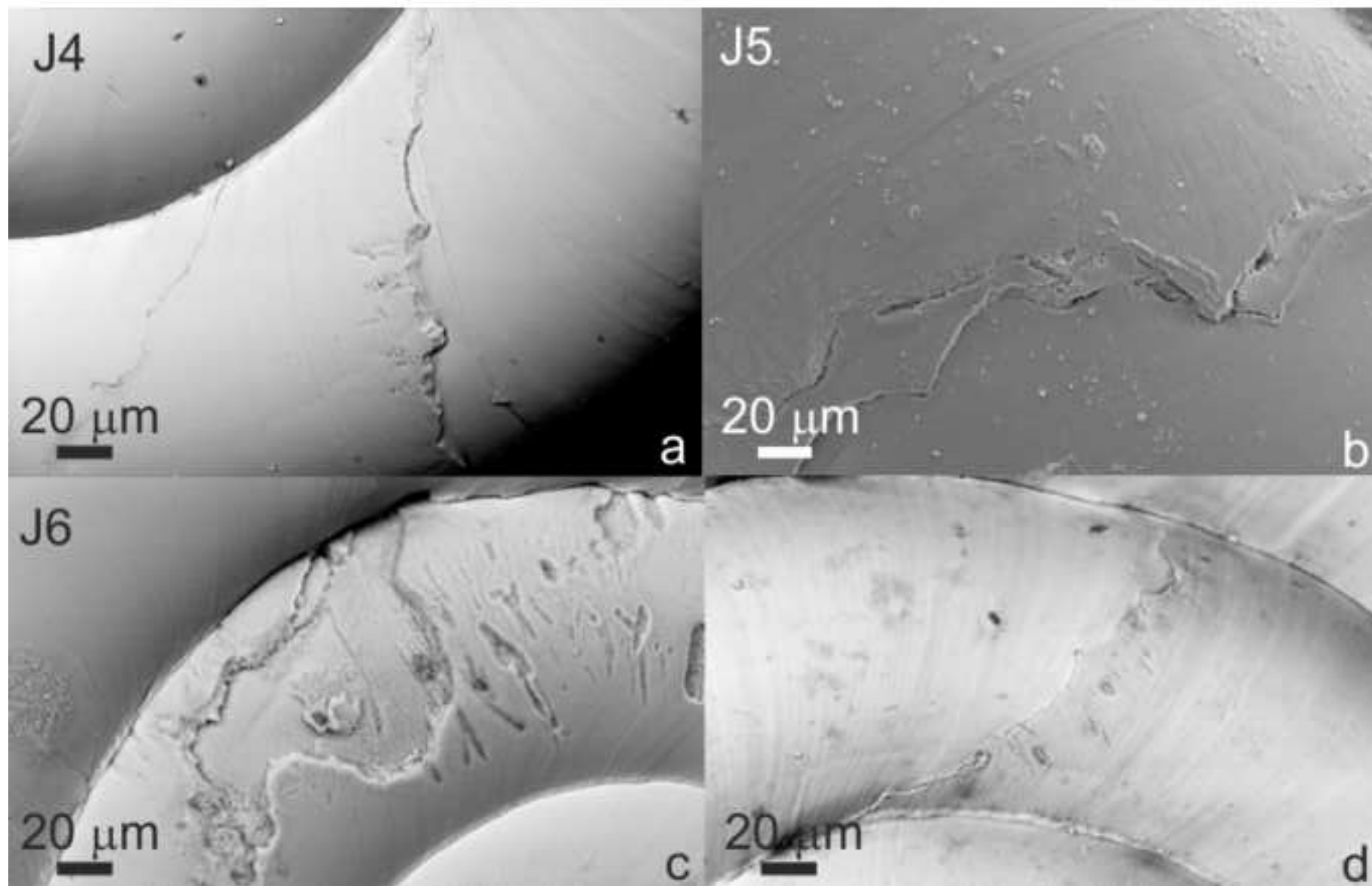


Fig 11

